ELSEVIER

Journal of Nuclear Materials 248 (1997) 27–33

journal of nuclear materials

# Retention and re-emission processes of hydrogen isotopes in graphite and beryllium

K. Morita *, B. Tsuchiya

*Department of Crystalline Materials Science, School of Engineering, Nagoya University, Furo-cho, Chikusa-ku, Nagoya 464-01, Japan*

**Abstract**

The mass balance equations and the rate constants of elementary processes related to retention and re-emission of hydrogen isotopes have been described for evaluation of their transient recycling fluxes from targets irradiated simultaneously with $H^+$ and $D^+$. The D/H ratios of the concentrations of H and D retained at steady state calculated under three different conditions are compared with the experimental values for graphite and beryllium measured by means of the elastic recoil detection technique. The retention and re-emission processes of hydrogen isotopes in graphite and beryllium are discussed. © 1997 Elsevier Science B.V.

## 1. Introduction

Evaluation and prediction of transient recycling fluxes of hydrogen isotopes from plasma-facing components are required in order to control the isotope ratio in the fueling during long-term burning D–T discharges. So far, the elementary processes related to their retention and re-emission have been extensively studied by many authors by means of different techniques. Data on retention and re-emission have been accumulated [1–3] and several models have been proposed [4–9]. For evaluation and prediction of the transient recycling fluxes, it is necessary to calculate time-dependent depth distributions of hydrogen isotopes retained in the wall materials and fluxes of atomic and molecular species produced through re-emission reactions from the depth distributions.

For their purpose, mass balance equations have been proposed by several authors [10–13], in which the retention and re-emission are described in terms of elementary processes, for instance, trapping, ion-induced and thermal detrapping, and local reactions of molecular recombination and hydrogen–target atom complex formation [11]. In the last two papers [12,13], the diffusion of hydrogen isotopes in crystallites of polycrystalline targets and their surface molecular recombination have been more exactly taken into account; this is the so called two-region-model [13]. The mass balance equations not including the diffusion term and the surface molecular recombination, but the local reaction of molecular recombination and hydrogen–target complex formation described in terms of the diffusion-limited reaction model can be regarded to be an approximation of the two-region-model, which are applicable for polycrystalline targets of small crystallites.

The rate constants of the elementary processes have been determined with the use of the mass balance equations for analysis of experimental data on retention mostly by independent implantation of H and D and re-emission by post-ion bombardment and thermal annealing. The diffusion-limited reaction model is very effective for extrapolation of the rate constants for $T$ from those for H and D using the isotope difference. It is also very promising for calculation of the rate constants for mixed molecular recombination and hydrogen–target atom complex formation which are of essential importance in simultaneous implantation of different hydrogen species. Recently, the present authors have found that there exists a large isotope difference between the concentrations of H and D retained in graphite at room temperature by simultaneous implantation

* Corresponding author. Tel.: +81-52 789 4686; fax: +81-52 789 3791; e-mail: k-morita@mail.nucl.nagoya-u.ac.jp.


*PII* S0022-3115(97)00113-X

with $H^+$ and $D^+$ ion beams. The isotope difference has been reasonably explained in terms of the mass balance equations with the rate constants of local mixed molecular recombination between an active species and a trapped one (H–D and D–H) expressed on the basis of the diffusion-limited reaction model [14]. Further application of the diffusion-limited reaction model to high temperature and other materials is very interesting.

In this paper, we discuss the experimental data on the isotope ratios of the concentrations of H and D retained in graphite and beryllium by simultaneous dual-beam ion implantation in comparison with the theoretical one calculated using the mass balance equations and compare the elementary processes in retention and re-emission in both materials which are ascribed to the difference between their isotope ratios.

## 2. Mass balance equations and the rate constants

### 2.1. Mass balance equations

The mass balance equations for estimation of the transient recycling fluxes of hydrogen isotopes are required to include several terms such as diffusion, implantation source, trapping, detrapping, molecular recombination and formation of hydrogen–target atom complex and recession of the surface. The targets implanted with energetic ions of hydrogen isotopes up to saturation (or a steady state) are heavily damaged and modified into complex textures which are composed of small crystallites of a few tens of nanometer in size for graphite and include small cavities, voids and bubbles for beryllium at room temperature. For such a situation, the two-region-model may be appropriate. The data analysis, however, is not straightforward. When the diffusion time in the small crystallites is smaller than the molecular recombination time and detrapping time, for simplicity, the diffusion-limited reaction model can be used for expression of the trapping, molecular recombination and hydrogen–target atom complex formation and the diffusion term may be dropped because the rate constants include the diffusion constants. For graphite in such a state, indeed the mass balance equations with local molecular recombination and local hydrocarbon formation have explained reasonably well the isothermal re-emission curves of H and D retained by independent ion implantation [15–18]. The mass balance equations may be applicable for beryllium in which the thermal re-emission rate is independent of the depth [19]. Therefore we extend the mass balance equations with the diffusion-limited reaction rate constant for calculating the concentrations of H and D atoms in targets under simultaneous $H^+$ and $D^+$ ion irradiation. A set of the mass balance equations for the local concentrations of activated (free) hydrogen isotopes ($n^H$ and $n^D$) and trapped ones ($n_T^H$ and $n_T^D$) are expressed in terms of the following equations:

$$\begin{aligned}\frac{dn^H}{dt} &= \Sigma_d^H n_T^H + \phi^H \sigma_d^{HH} n_T^H + \phi^D \sigma_d^{DH} n_T^H \\ &\quad - \Sigma_T^H \left(C_0 - n_T^H - n_T^D\right) n^H - K^{HH} n^H n_T^H \\ &\quad - K^{HD} n^H n_T^D - 2K_1^{HH} n^H n^H - K_1^{HD} n^H n^D \\ &\quad - \alpha R^H n_T^H n^H - \alpha R^H n_T^D n^H + \frac{\phi^H}{\Delta R^H}, \end{aligned} \tag{1}$$

$$\begin{aligned}\frac{dn_T^H}{dt} &= -\Sigma_d^H n_T^H - \phi^H \sigma_d^{HH} n_T^H - \phi^D \sigma_d^{DH} n_T^H \\ &\quad + \Sigma_T^H \left(C_0 - n_T^H - n_T^D\right) n^H - K^{HH} n^H n_T^H \\ &\quad - K^{DH} n^D n_T^H - \alpha R^H \beta^H n_T^H n^H - \alpha R^D \beta^H n_T^H n^D, \end{aligned} \tag{2}$$

$$\begin{aligned}\frac{dn^D}{dt} &= \Sigma_d^D n_T^D + \phi^H \sigma_d^{HD} n_T^D + \phi^D \sigma_d^{DD} n_T^D \\ &\quad - \Sigma_T^D \left(C_0 - n_T^H - n_T^D\right) n^D - K^{DD} n^D n_T^D \\ &\quad - K^{DH} n^D n_T^H - 2K_1^{DD} n^D n^D - K_1^{HD} n^D n^H \\ &\quad - \alpha R^D n_T^D n^D - \alpha R^D n_T^H n^D + \frac{\phi^D}{\Delta R^D}, \end{aligned} \tag{3}$$

$$\begin{aligned}\frac{dn_T^D}{dt} &= -\Sigma_d^D n_T^D - \phi^H \sigma_d^{HD} n_T^D - \phi^D \sigma_d^{DD} n_T^D \\ &\quad + \Sigma_T^D \left(C_0 - n_T^H - n_T^D\right) n^D - K^{DD} n^D n_T^D \\ &\quad - K^{HD} n^H n_T^D - \alpha R^D \beta^D n_T^D n^D - \alpha R^H \beta^D n_T^D n^H, \end{aligned} \tag{4}$$

where $C_0$ is the trap concentration, $\phi^H$ and $\phi^D$ are the implantation fluxes of $H^+$ and $D^+$, $\phi^H/\Delta R^H$ and $\phi^D/\Delta R^D$ are the source terms of $H^+$ and $D^+$ ions ($\Delta R^H$ and $\Delta R^D$ represent the range straggling for $H^+$ and $D^+$ ions), $\sigma_d^{HH}$ and $\sigma_d^{HD}$ are the $H^+$ ion-induced detrapping cross-sections for trapped H and D atoms and $\sigma_d^{DH}$ and $\sigma_d^{DD}$ are the $D^+$ ion-induced detrapping cross-sections for trapped H and D atoms, $\Sigma_T^H$ and $\Sigma_T^D$ are the trapping rate constants for H and D atoms, $\Sigma_d^H$ and $\Sigma_d^D$ are the thermal detrapping rate constants for trapped H and D atoms, $K^{HH}$, $K^{DD}$, $K^{HD}$ and $K^{DH}$ represent the rate constants of local molecular recombination between a mobile species and a trapped one in the form of $H_2$, $D_2$ and HD, respectively. $K_1^{HH}$, $K_1^{DD}$ and $K_1^{HD}$ represent the rate constants of molecular recombination between mobile hydrogen isotopes also in the form of $H_2$, $D_2$ and HD, respectively. $R^H$ and $R^D$ are the rate constants of hydrocarbon formation for mobile H and D atoms to be trapped into a precursor of hydrogen–target complex molecule, $\alpha$ is the fraction of the number of precursors to that of total trapped hydrogen atoms and $\beta^H$ and $\beta^D$ represent the numbers of H and D atoms in the precursor. The break-up of methane by incident ions, observed recently by Haasz et al. [20,21], is taken into account indirectly via ion-induced

detrapping of trapped hydrogen atoms in the precursor. Thus, $\alpha$ is the steady state value. The atomic re-emission of hydrogen is not taken into account, because the experiments are below 900 K.

### 2.2. The rate constants for elementary processes

In order to calculate the transient recycling fluxes from the solution of the mass balance equations described above, all the rate constants for elementary processes need to be determined from the analysis of experimental data using the corresponding mass balance equations, or from theoretical calculation using a definite model. The present authors have determined them from analysis of the experimental data on post ion bombardment, isotope replacement and isothermal annealing of hydrogen isotopes retained mostly in graphite [15–18] and partly in beryllium by independent ion implantation of H and D [19]. All the rate constants except $\alpha$, $\beta^{H}$ and $\beta^{D}$ are briefly described with expressions based on the diffusion-limited reaction model.

#### 2.2.1. Diffusion constant

The experimental depth profiles of H retained in graphite at steady state by implantation with 5 keV $H_2^+$ ions at different fluxes and at different temperatures were analyzed with the use of the mass balance equations in the two-region-model [12]. The diffusion constant of H in isotropic graphite (IG110U) was determined to be $D^{H} = 1.1 \times 10^{-13} \exp(-0.20\ \mathrm{eV}/kT)\ (\mathrm{cm}^2/\mathrm{s})$.

#### 2.2.2. Trapping rate constant

The steady-state concentrations of H and D retained in graphite and beryllium by ion implantation at room temperature were found to be 0.4–0.5 in fraction to the target density. This fact indicates that the trapping rate constant in both materials is extremely high compared with the other rate constants related to the re-emission. However, the value of the trapping rate constant has never been directly measured. The rate constant is expressed by $\Sigma_T^{H} = 4\pi r_T D^{H} C_0 \eta^{H}$ in the diffusion-limited reaction model, where $C_0$ is the trap density, $D^{H}$ is the diffusion constant, $r_T$ is the effective radius for trapping and $\eta^{H}$ is the trapping probability for H.

#### 2.2.3. Thermal detrapping rate constant

Thermal detrapping rate constants of H and D in graphite and beryllium were determined from the decay curves obtained on post-isothermal annealing of specimens loaded up to saturation by independent ion implantation. It follows that $\Sigma_d^{H} = 5.6 \exp(-0.60\ \mathrm{eV}/kT)\ (\mathrm{s}^{-1})$ and $\Sigma_d^{D} = 4.0 \exp(-0.60\ \mathrm{eV}/kT)\ (\mathrm{s}^{-1})$ for graphite [17] and $\Sigma_d^{D} = 7.5 \times 10^{-2} \exp(-0.14\ \mathrm{eV}/kT)\ (\mathrm{s}^{-1})$ for beryllium [19].

#### 2.2.4. Ion-induced detrapping cross-sections

The detrapping cross-sections of H by $D^+$ and D by $H^+$ in graphite were determined from analysis of the experimental data on re-emission of H by $D^+$ bombardment and D by $H^+$ bombardment to be $\sigma_d^{DH} = 3.3 \times 10^{-18}$ $\mathrm{cm}^2$ at 2 keV and $\sigma_d^{HD} = 2.5 \times 10^{-18}$ $\mathrm{cm}^2$ at 2.5 keV, respectively. The detrapping cross-sections of H by $H^+$ and D by $D^+$ are extrapolated to be $\sigma_d^{HH}$ and $\sigma_d^{DD} = 2.9 \times 10^{-18}$ $\mathrm{cm}^2$ from the theoretical mass dependence calculated from the differential cross-sections of the hydrogen–hydrogen momentum transfer collision [16].

#### 2.2.5. Local molecular recombination rate constants between an activated species and a trapped one

The local molecular recombination rate constants between an activated hydrogen and a trapped one were determined from the analysis of the peak concentrations of H retained in graphite at steady state by implantation with 5 keV $H_2^+$ at different fluxes and at different temperatures [12]. It follows that $K^{HH} = 6 \times 10^{-21} \exp(-0.25\ \mathrm{eV}/kT)$ $(\mathrm{cm}^3/\mathrm{s})$.

The ratios of the local molecular recombination rate constant to the trapping rate constant in graphite were determined from the analysis of MeV $He^+$ ion-induced re-emission of hydrogen isotopes to be $K^{HH}/\Sigma_T^{H} = 0.2$ and $K^{DD}/\Sigma_T^{D} = 0.1$ [15]. The rate constants are expressed in the diffusion-limited reaction model to be $K^{HH} = 4\pi r_R^{H} D^{H} \xi^{HH}$ and $K^{DD} = 4\pi r_R^{D} D^{D} \xi^{DD}$, where $r_R^{H}$ and $r_R^{D}$ are the effective radii for recombination with trapped H and D; $\xi^{HH}$ and $\xi^{DD}$ are the recombination probability for H–H and D–D. The expressions for $\Sigma_T$ and $K$ explain reasonably well the isotope difference between $K^{HH}/\Sigma_T^{H}$ and $K^{DD}/\Sigma_T^{D}$.

#### 2.2.6. Local molecular recombination rate constants between activated species

The local molecular recombination rate constants $K_1$ between thermally activated species in graphite were determined from the analysis of the decay curves obtained on post-isothermal annealing of specimens loaded up to saturation by independent implantation [18]. The values of $(K_1^{HH}/C_0)\,(\Sigma_d^{H}/\Sigma_T^{H})^2$ and $(K_1^{DD}/C_0)\,(\Sigma_d^{D}/\Sigma_T^{D})^2$ were determined to be $45 \exp(-1.2\ \mathrm{eV}/kT)\ (\mathrm{s}^{-1})$ and $18 \exp(-1.2\ \mathrm{eV}/kT)\ (\mathrm{s}^{-1})$, respectively. According to the diffusion-limited reaction model, it follows that $K_1^{HH} = 4\pi r_{HH} D^{H} \xi^{HH}$, $K_1^{DD} = 4\pi r_R^{DD} D^{D} \xi^{DD}$ and $K_1^{HD} = 4\pi r_R^{HD} D^{HD} \xi^{HD}$, where $r_R^{ij}$ are the effective radii for recombination between mobile species $i$ and $j$ given by a factor of $2\sqrt{(D^i + D^j)\tau}$, where $\tau$ is the characteristic time, $\xi^{ij}$ is the formation probability for a molecule $ij$ and $D^{HD} = (D^{H} + D^{D})/2$. The expressions explain reasonably well the isotope difference between $(K_1^{HH}/C_0)(\Sigma_d^{H}/\Sigma_T^{H})^2$ and $(K_1^{DD}/C_0)(\Sigma_d^{D}/\Sigma_T^{D})^2$.

#### 2.2.7. Hydrogen–target complex formation rate constant

The rate constants for hydrogen–target atom complex formation were taken into account for evaluating the contribution of methane formation (emission) to the re-emission of hydrogen isotopes by isothermal annealing [18]. The rate constant for methane formation is expressed as $R^{H} = 4\pi r_{HC} D^{H} \eta^{H}$ and $R^{D} = 4\pi r_{HC} D^{D} \eta^{D}$ in the diffu-

sion-limited reaction model, where $r_{HC}$ is the effective radius of the precursor and $\eta^H$ and $\eta^D$ are the probabilities for H and D to be trapped into the precursor, similar to the trapping rate constant.

## 3. The isotope (D/H) ratio of the steady-state concentrations of H and D retained under simultaneous $H^+$ and $D^+$ irradiation

### 3.1. Calculations

#### 3.1.1. Low temperature (small diffusion constant)

At room temperature, the contribution of thermally activated processes, such as thermal detrapping, molecular recombination between activated species and formation of hydrogen–target complexes, is significantly small so it may be neglected. The re-emission of trapped species only takes place through local molecular recombination with species activated due to ion-induced detrapping, which are energetic and a-thermal. The D/H ratio at steady-state is expressed by the following equation as a solution of the mass balance equations [14],

$$\frac{N_T^H}{n_T^D} = \left[\left(\frac{K^{DD}}{\Sigma_T^D}\right)\Big/\left(\frac{K^{HH}}{\Sigma_T^H}\right)\right] \times \left\{1 + \frac{\Delta R^D}{\Delta R^H}\frac{\phi^H}{\phi^D} + 2\left(\sigma_d^{DD} + \sigma_d^{HD}\frac{\phi^H}{\phi^D}\right) n_T^D \Delta R^D\right\} \Big/ \left\{1 + \frac{\Delta R^H}{\Delta R^D}\frac{\phi^D}{\phi^H} + 2\left(\sigma_d^{HH} + \sigma_d^{DH}\frac{\phi^D}{\phi^H}\right) n_T^H \Delta R^H\right\}. \quad (5)$$

The value of $n_T^H/n_T^D$, calculated self-consistently from Eq. (5) using the above-described rate constants and experimental condition $\Delta R^H/\Delta R^D = 0.8$ and $\phi^H/\phi^D = 1$ described later, was 1.5.

#### 3.1.2. Low temperature (large diffusion constant)

At low temperature, we also consider that the hydrogen re-emission takes place due to local molecular recombination between free species activated by ion bombardment because of a large diffusion constant. Such a case may correspond to hydrogen behavior in beryllium which is modified into the complex textures described above by the implantation up to saturation (or a steady-state). Since the detrapping takes place due to ion bombardment, the ratio of H and D retained at room temperature and at $\phi^H = \phi^D$ is expressed, as a solution of Eqs. (1)–(4) at steady state,

$$\frac{\Delta R^H}{\Delta R^D} = \left[2K_1^{HH}\left(\frac{\sigma_d^H}{\Sigma_T^H}\right)^2 x^2 + K_1^{HD}\left(\frac{\sigma_d^H}{\Sigma_T^H}\right)\left(\frac{\sigma_d^D}{\Sigma_T^D}\right) x\right] \Big/ \left[2K_1^{DD}\left(\frac{\sigma_d^D}{\Sigma_T^D}\right)^2 + K_1^{HD}\left(\frac{\sigma_d^H}{\Sigma_T^H}\right)\left(\frac{\sigma_d^D}{\Sigma_T^D}\right) x\right], \quad (6)$$

where $x = n_T^H/n_T^D$, $\sigma_d^H = \sigma_d^{HH} + \sigma_d^{DH}$, $\sigma_d^D = \sigma_d^{DD} + \sigma_d^{HD}$. Using the above-described rate constants, the ratio $n_T^H/n_T^D$ is expressed by the following equation:

$$\frac{n_T^H}{n_T^D} = \sqrt{K_1^{DD}\left(\frac{\sigma_d^D}{\Sigma_T^D}\right)^2 \Big/ K_1^{HH}\left(\frac{\sigma_d^H}{\Sigma_T^H}\right)^2} \times \left(\sqrt{1 + \frac{(1-f)^2}{16}\frac{(K_1^{HD})^2}{K_1^{HH}K_1^{DD}}} - \frac{(1-f)}{4}\right) \times \frac{K_1^{HD}}{\sqrt{K_1^{HH}K_1^{DD}}}, \quad (7)$$

where $f = \Delta R^D/\Delta R^H$ which is 1.25 in the present experiment.

The isotope ratio for H and D of $K_1^{ii}(\sigma_d^i/\Sigma_T^i)^2$ in graphite is available. In such a case, the ratio $n_T^D/n_T^H$ is estimated to be 1.25.

#### 3.1.3. Elevated temperature

At elevated temperatures, the retained concentrations of hydrogen isotopes decrease due to an increase of the rate constants of thermally activated processes for re-emission such as thermal detrapping, local molecular recombination between thermally activated species and hydrogen–target complex, for instance, which are major processes at temperatures above 700 K when the implantation flux is small so that the ion-induced detrapping rate is neglected. Under such a condition, the ratio of D to H retained at steady state is expressed by the following equation:

$$f = \left\{\left[2k_{eff}^{HH} + \alpha\left(1+\beta^H\right)\Sigma_d^H\right]x^2 + \left[k_{eff}^{HD} + \alpha\Sigma_d^H + \alpha\beta^H\Sigma_d^D\right]x\right\} \times \Big/\left\{\left[2k_{eff}^{DD} + \alpha\left(1+\beta^D\right)\Sigma_d^D\right] + \left[k_{eff}^{HD} + \alpha\Sigma_d^D + \alpha\beta^D\Sigma_d^H\right]x\right\}, \quad (8)$$

where

$$k_{eff}^{ij} = \frac{K_1^{ij}}{C_0}\left(\frac{\Sigma_d^i}{\Sigma_T^i}\right)\left(\frac{\Sigma_d^j}{\Sigma_T^j}\right),$$

$f = \Delta R^H/\Delta R^D$ ($\equiv 1.25$) and $x = n_T^H/n_T^D$. For the derivation, it was assumed that $r_{CH} = r_T$, namely $R^H = \Sigma_T^H$ and $R^D = \Sigma_T^D$ and $C_0 \gg n_T^H + n_T^D$. The values of $2(K_1^{ii}/C_0)(\Sigma_d^i/\Sigma_T^i)^2$ are three orders of magnitude smaller than the value of $\Sigma_d^i$, as described above for graphite. Since it was also experimentally shown that $\Sigma_T^H = \Sigma_T^D = \sqrt{2}$ [17], it follows that

$$\left(1+\beta^H\right)\sqrt{2}\,x^2 + \left[\left(\sqrt{2}+\beta^H\right) - f\left(1+\beta^D\sqrt{2}\right)\right]x - f\left(1+\beta^D\right) = 0. \quad (9)$$

This equation indicates that the value of $x$ can be determined from the value of $\beta^H$ and $\beta^D$ and vice versa. We have no data on $\beta^H$ and $\beta^D$ yet. The values of $\beta^H$ and

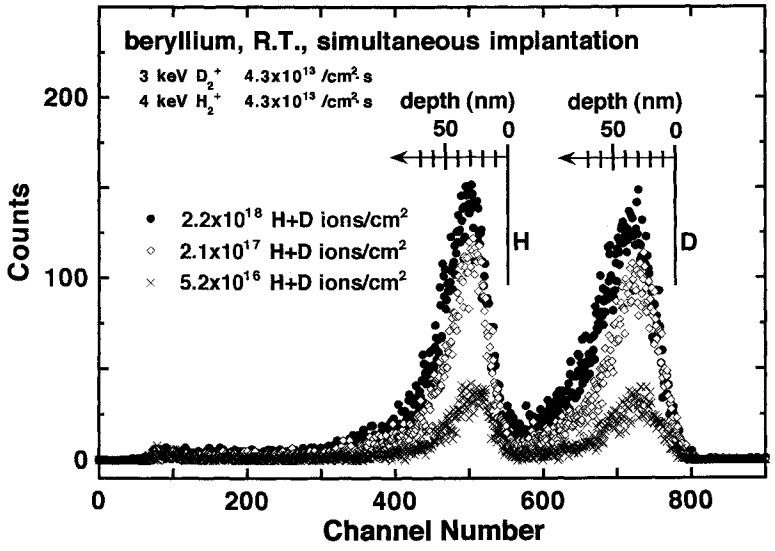


Fig. 1. ERD spectra from beryllium measured at several stages of simultaneous irradiation with 3 keV $D_2^+$ and 4 keV $H_2^+$ at room temperature, where depth scale is shown.

$\beta^D$ are calculated to be 2.1 and 0.9, respectively for $x = 1.5$, which is equal to the room temperature value.

### 3.2. Experiments

The graphite specimen used was an isotopic graphite plate (IG110U) of $10 \times 15 \times 1$ mm$^3$ in size. In the case of beryllium, a disc (99 at.% in purity from Bruch–Wellman) of 30 mm diameter and 1 mm thickness was used. The oxygen content in the beryllium specimen measured by Rutherford backscattering spectroscopy (RBS) was 0.93%, little heavier impurities were also present in the bulk.

The graphite and beryllium specimens were irradiated simultaneously with 4 keV $H_2^+$ and 3 keV $D_2^+$ ions at angles of 20° and 35° to the surface normal, respectively, so that the peak depths of both ions in the target coincided with each other [14]. The implantation flux of the $H^+$ and $D^+$ ions on the target were $4.3 \times 10^{13}$ ions/cm$^2$ s. The implantation temperature of beryllium was room temperature and that of graphite ranged from 300 to 900 K. The concentrations of H and D retained in the specimens were measured after several stages of implantation by means of elastic recoil detection (ERD) with a 1.7 MeV $He^+$ beam. The $He^+$ fluence was simultaneously monitored by means of the RBS technique.

Typical ERD spectra from beryllium irradiated simultaneously at room temperature with 3 keV $D_2^+$ and 4 keV $H_2^+$ ions are shown in Fig. 1, where the depth scales for H and D are inserted. The ERD spectra are qualitatively the

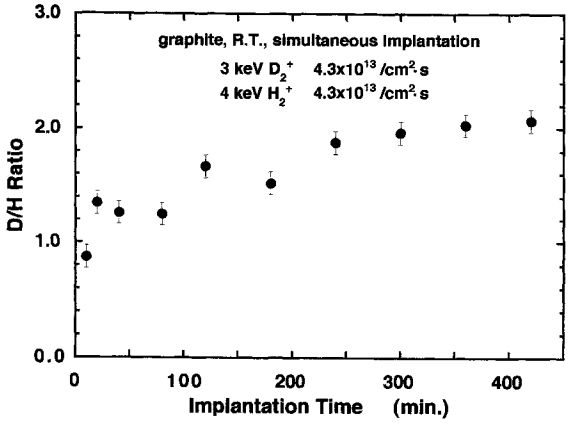


Fig. 2. The D/H ratio of concentrations of H and D retained in graphite, by simultaneous irradiation with 3 keV $D_2^+$ and 4 keV $H_2^+$ at room temperature, as a function of implantation time.

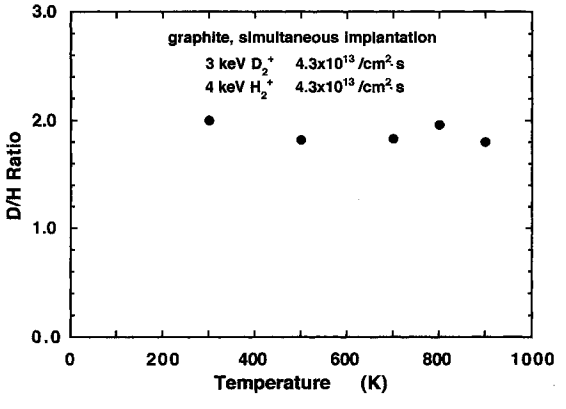


Fig. 3. Temperature dependence of the D/H ratio of the concentrations of H and D retained in graphite at steady-state by simultaneous irradiation with 3 keV $D_2^+$ and 4 keV $H_2^+$.

Table 1
The D/H ratio of the concentrations of H and D retained in graphite and beryllium irradiated simultaneously with 3 keV $D_2^+$ and 4 keV $H_2^+$ ions

| | D/H ratio | | | | Major processes for re-emission | |
|---|---|---|---|---|---|---|
| | experiments | | calculations | | C | Be |
| | C | Be | C | Be | | |
| Room temperature | 2.0 | | 1.5 | | $K$, $\sigma_d\phi$ | |
| | | 1.2 | | 1.25 | | $K_1$, $\sigma_d\phi$ |
| Elevated temperature | | | 1.3 | | $K_1$, $\Sigma_d$ | |
| | 1.8 | – | 1.5 | | $K_1$, $R$, $\Sigma_d$ ($\beta^H/\beta^D = 2.1/0.9$) | |

$K$: local molecular combination between an activated species and a trapped one. $K_1$: local molecular recombination between activated species. $R$: hydrocarbon molecule formation (methane). $\sigma_d\phi$: ion-induced detrapping. $\Sigma_d$: thermal detrapping.

same as the depth profiles of H and D retained in beryllium, which reflect the damage profiles in beryllium induced by 2 keV $H^+$ and 1.5 keV $D^+$ ions. The ERD spectra from graphite were found to show almost the same profiles, but with extra diffusion tail extending to deeper layers [14]. It is seen from Fig. 1 that both peaks of H and D separate well from each other and both peak heights increase as the implantation fluences increase. The relative concentrations of H and D were calculated form the counts of H and D averaged over 40 channels around the peaks by standard analysis techniques. Since the peak depths of H and D from the target surface are the same, the error in the D/H ratio is estimated to be less than 10%, which is mainly ascribed to uncertainty in the recoil cross-sections.

*3.2.1. Graphite*

The D/H ratios of the concentrations of H and D retained in graphite at room temperature are shown as a function of the implantation fluence in Fig. 2; the D/H ratio increases gradually from unity and saturates at ~ 2 as the fluence increases.

Similar measurements were done at temperatures of 500, 700, 800 and 900 K. The dependence of the D/H ratio on the temperature is shown in Fig. 3; the D/H ratio is almost independent of the temperature. For comparison with the theoretical calculations, the values of the D/H ratio at saturation are tabulated in the low and elevated temperature regions (see Table 1).

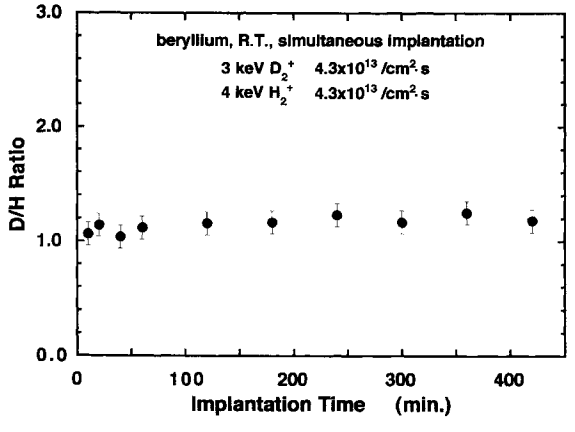


Fig. 4. The D/H ratio of concentrations of H and D retained in beryllium, by simultaneous irradiation with 3 keV $D_2^+$ and 4 keV $H_2^+$ at room temperature, as a function of implantation time.

*3.2.2. Beryllium*

The D/H ratio of the concentrations of H and D retained in beryllium at room temperature is shown as a function of the fluence in Fig. 4. It is seen from Fig. 4 that the D/H ratio increases gradually from unity and saturates at ~ 1.2 as the fluence increases. The value of the D/H ratio at saturation is also shown in Table 1.

## 4. Discussion

The calculations and the experiments on the D/H ratio of the concentrations of H and D retained at steady state by simultaneous irradiation with $H^+$ and $D^+$ ions have been summarized in Table 1. It is seen from Table 1 that the calculated values of the D/H ratio at room temperature are in good agreement with the experimental values. In the calculation, the diffusion term was neglected for simplicity, which would expect to reduce the absolute steady-state concentration of H more than that of D. Thus, the small difference between the experimental and calculated ratios is ascribed to dropping of the diffusion term from the mass balance equations.

It is also seen from Table 1 that the calculated value of the D/H ratio at elevated temperature, on the assumption of no hydrocarbon emission, becomes lower than the value at room temperature. Thus, we took into account the methane emission. However, we have no data of $\beta^H$ and $\beta^D$. There is only one measurement of mixed-isotope methane emission during simultaneous $H^+$ and $D^+$ bombardment by Chiu and Haasz [22]; however, we can not extract the values of $\beta^H$ and $\beta^D$ from their data. Therefore, we found the values of $\beta^H$ and $\beta^D$ to be 2.1 and 0.9 for $n_T^D/n_T^H = 1.5$, using Eq. (9) and $\beta^H + \beta^D = 3$ for

methane formation. This fact might indicate that the H/D ratio in the precursor is no less than 2.1/0.9.

As shown in the previous section, we have little data on beryllium which are applicable to the mass balance equations. On the other hand, the theoretical expression of the D/H concentration ratio at steady-state depends mostly on the D/H ratio in the rate constants of elementary processes as seen from Eq. (6). When the rate constants are expressed classically in the diffusion-limited reaction model, it is expected that the D/H ratio in the rate constants is not dependent on D, but effective radii $r_T$ and $r_R$ and reaction probabilities $\eta$ and $\zeta$ which are almost independent of the target materials. The value of the D/H concentration ratio for beryllium at steady-state at room temperature calculated from Eq. (6) using the data for graphite was found to be 1.25, which agrees well with the experimental D/H ratio for beryllium at room temperature. This fact seems to indicate that the diffusion-limited reaction model is effective. Finally, it is noted that the rate constants of elementary processes for hydrogen retention and re-emission in beryllium are needed.

## 5. Summary

The mass balance equations and the rate constants of elementary processes related to retention and re-emission of hydrogen isotopes have been described for evaluation of their transient recycling fluxes form targets irradiated simultaneously with $H^+$ and $D^+$.

The D/H ratios of the concentrations of H and D retained at steady state have been calculated under three different conditions: (1) room temperature and local molecular recombination between activated species and trapped ones, (2) room temperature and local molecular recombination between activated species, and (3) elevated temperature, local molecular recombination between activated species and hydrogen–target complex formation. The D/H ratio has been found to depend on the isotope ratio of the rate constants for relevant elementary processes. Since the isotope ratio of the rate constants is almost independent of the target material in the diffusion-limited reaction model, the D/H ratio is not dependent on the material if the re-emission processes are the same.

The experimental D/H ratio for graphite at room temperature and at $\phi^H = \phi^D$ was found to be 1.8, which agrees well with the theoretical value of 1.5 calculated under condition (1). The experimental D/H ratio for beryllium at room temperature and at $\phi^H = \phi^D$ was found to be 1.2, which agrees well with the theoretical value under the condition (2). The experimental D/H ratios for graphite at elevated temperatures were found to be temperature-independent and 1.8, which is a little bit larger than the theoretical value of 1.3 under condition (3), without hydrocarbon molecule formation. Finally, it is noted that for consideration of hydrocarbon molecule formation, data on the numbers of H and D included in the precursor for hydrocarbon formation are needed.

## References

[1] W. Möller, J. Nucl. Mater. 162–164 (1989) 138.
[2] R.A. Causey, J. Nucl. Mater. 162–164 (1989) 151.
[3] K.L. Wilson et al., Nucl. Fusion (Suppl.) 1 (1991) 31.
[4] W. Möller, B.M.U. Scherzer, Appl. Phys. Lett. 50 (1987) 1870.
[5] Ch. Wild, P. Koidl, Appl. Phys. Lett. 51 (1987) 1506.
[6] K. Morita, Y. Hasebe, J. Nucl. Mater. 176&177 (1990) 213.
[7] W.R. Wampler, J. Nucl. Mater. 122&123 (1984) 213.
[8] W.R. Wampler, J. Nucl. Mater. 196–198 (1992) 983.
[9] J. Roth, J. Bohdansky, Appl. Phys. lett. 51 (1987) 13.
[10] W. Möller, B.M.U. Sckerzer, J. Appl. Phys. 64 (1988) 4860.
[11] K. Morita, Y. Hasebe, Mem. Fac. Eng. Nagoya Univ. 45 (1993) 57.
[12] K. Morita, K. Ohtsuka, Y. Hasebe, J. Nucl. Mater. 162–164 (1989) 990.
[13] A.A. Haasz, P. Franzen, J.A. Davies, S. Chiu, C.S. Pitcher, J. Appl. Phys. 77 (1995) 66.
[14] B. Tsuchiya, K. Morita, J. Nucl. Mater. 227 (1996) 195.
[15] B. Tsuchiya, K. Morita, J. Nucl. Sci. Technol. 31 (1994) 1301.
[16] B. Tsuchiya, K. Morita, J. Nucl. Mater. 226 (1995) 298.
[17] K. Morita, Y. Muto, J. Nucl. Mater. 196–198 (1992) 963.
[18] Y. Muto, K. Morita, J. Nucl. Mater. 223 (1995) 262.
[19] B. Tsuchiya, K. Morita, J. Nucl. Mater. (1996) in press.
[20] S. Chiu, A.A. Haasz, P. Franzen, J. Nucl. Mater. 218 (1995) 319.
[21] A.A. Haasz, P. Franzen, J. Nucl. Mater. 220–222 (1995) 815.
[22] S. Chiu, A.A. Haasz, J. Nucl. Mater. 208 (1994) 282.